博 士 論 文

Synthesis and antibacterial photodynamic assessments of lysozyme-Au nanoclusters/rose bengal conjugate
（リゾチーム金ナノクラスター/ローズベンガル複合体の合成と光線力学的評価）

令和２年３月申請

北海道大学

大学院歯学研究科口腔医学専攻

岡　本　一　絵

Synthesis and antibacterial photodynamic assessments of lysozyme-Au nanoclusters/rose bengal conjugate

Ichie OKAMOTO

Institutions

Department of Periodontology and Endodontology, Graduate School of Dental Medicine,

Hokkaido University

N13, W7, Kita-ku, Sapporo, 060-8586, Japan.

Key words

Antibacterial photodynamic therapy (aPDT), *Porphyromonas gingivalis,* Resonance energy transfer (RET), Singlet oxygen, *Streptococcus mutans,* White light emitting diode (LED).

Abstract

Antibacterial photodynamic therapy (aPDT) is anticipated for reducing infection via generation of singlet oxygen ($^1O_2$) against dental diseases, instead of antibiotic therapy. Reportedly, Au nanoclusters (Au NCs) showed the properties of aPDT effects and biosafety. To promote the antibacterial effect of aPDT using Au NCs, we synthesized lysozyme-Au NCs/rose bengal (Lys-Au NCs/RB) conjugate as a novel photosensitizer. It is expected the reduction of bacterial growth by antibacterial protein, Lys and enhancement of $^1O_2$ generation related to resonance energy transfer (RET) mechanism with Au NCs/RB conjugate. Accordingly, we characterized Lys-Au NCs/RB irradiated with white light emitting diode (LED) and assessed the antibacterial and biosafe effect of photoexcited Lys-AuNCs/RB.

$^1O_2$ generation of Lys-Au NCs/RB irradiated with white LED (420~750 nm) was detected by a methotrexate (MTX) probe. UV–Vis absorption spectroscopy and steady-state fluorescence spectroscopy measurements were performed to confirm the RET process in the Lys-Au NCs/RB. Subsequently, the antibacterial effects of photoexcited Lys-Au NCs/RB was assessed by bacterial growth experiments, live/dead staining and

morphological observations using oral bacterial cells. In addition, the biosafety of Lys-Au NCs/RB was examined using NIH3T3 mammalian cells.

We confirmed the $^1O_2$ generation ability of Lys-Au NCs/RB using the $^1O_2$ detection probe. The fluorescent lifetime measurements demonstrated that the RET process likely occur from the Au NCs to the RB in Lys-Au NCs/RB. Antibacterial activity of Lys-Au NCs/RB was significantly greater than that of Lys-Au NCs alone or RB alone ($P<0.01$). In addition, Lys-Au NCs/RB reduced the bacterial turbidity of both gram positive and negative bacterial cells. Bacterial cells were morphologically damaged by application of photoexcited Lys-Au NCs/RB. Furthermore, photoexcited Lys-Au NCs/RB increased red fluorescence (indicating dead cells) of in vitro biofilm of *S. mutans.* However, photoexcited Lys-Au NCs/RB did not negatively affect the adhesion, spreading, and proliferation of mammalian cells. In conclusion, Lys-Au NCs/RB conjugate exhibited aPDT activity to be beneficial for dental treatment.

1. Introduction

Antibacterial photodynamic therapy (aPDT) is widely investigated for the treatment of oral infections, such as endodontic disease, periodontitis and peri-implantitis. Use of conventional antibiotics have problems to promote the bacterial drug resistance[1] and allergy. In addition, bacterial biofilm formed on the tooth surface frequently defends the drug penetration into biofilm[2]. In aPDT, exciting photosensitizers generates singlet oxygen ($^1O_2$) and exerts an antibacterial effect to kill or control gram positive and negative bacterial cells[3,4]. In contrast to antibiotic therapy, aPDT rarely produces drug-resistant bacteria and possibility destroy the biofilm matrix[5-9]. Thus, aPDT should be developed as an effective antibacterial treatment to solve the problems of conventional antibiotic therapy in dental field.

Organic dye, such as methylene blue (MB) and rose bengal (RB), reportedly employed for the substrate for photoexcitation in aPDT[10]. Organic photosensitizers show high antibacterial activities, however, they require the narrow band of excitation wavelength (650 to 800 nm) to generate $^1O_2$[11]. Kawasaki et al. previously reported that $Au_{25}(SR)_{18}$– nanoclusters (H−SR = captopril) (Au NCs) showed to create $^1O_2$ as the photodynamic effects. Au NCs has physical advantages regarding widely adsorption wavelength (400 to 900 nm) for photoexcitation[12]. Furthermore, Miyata et al. revealed that Au NCs exhibited the good cytocompatibility, as well as antibacterial effects, when compared to conventional organic dye[12]. Hence, it is expected that novel photosensitizer including Au NCs would be developed for aPDT.

Resonance energy transfer (RET) is widely known as the phenomenon of energy transfer between two light-sensitive molecules[13]. Yamamoto et al. created a photosensitizer composed of Au NCs and MB and showed the evidence of occurrence of RET[14]. It was suggested that the light energy absorbed by the Au NCs was transferred to MB to generate a large amount of $^1O_2$. The complex of Au NCs and organic dye may absorb the visible light wavelength, like white LED, to effectively promote the generation of $^1O_2$ through the RET mechanism. In this study, we created novel photosensitizer Au NCs protected by lysozyme (Lys) and RB as the photosensitive dye.

The strategies of Lys-Au NCs/RB conjugate are shown as follow; Lys is known as a powerful antibacterial protein widely distributed in various biological media and tissues[15]. Recently, the effect of Lys on reducing biofilms was demonstrated[16]. Thus, the composite of photosensitizer, RB with Lys would have advantages on increased aPDT action and the reduction of biofilms, compared to RB alone. Moreover, RET process from Au NCs to RB is expected in the Lys-Au NCs/RB, since the donor (AuNCs) emission and the acceptor (RB) absorption spectra are overlapping; such RET process enhances the aPDT activity of RB[14]. We evaluated in this study whether Lys-Au NCs/RB with white LED light irradiation exerted antibacterial activity against oral bacteria, in particular, supported by RET mechanism. In addition, the assessment of cytotoxicity of Lys-Au NCs/RB was evaluated against mammalian cells to elucidate biosafe properties for clinical setting.

2. Materials and Methods

2.1 Materials

All the chemicals were used as received without further purification. Tetrachloroauric(III) acid ($HAuCl_4 \cdot 3H_2O$, 99.99%), methotrexate (MTX, 98%), dimethylformamide (DMF, 99.5%), Lys (for Biochemistry, from Egg White), methanol (99.9%), RB, and heavy water (D_2O, 99.9%) were purchased from FUJIFILM Wako Pure Chemical Corporation, Osaka, Japan. Nanopure water (resistivity: 18.2 MΩ·cm) was obtained using a Barnstead NANO pure DI water system (Cole-Parmer Instrument Company, Vernon Hills, IL, USA).

2.2 Synthesis of Lyz-Au NCs

The synthesis of Lyz-Au NCs was performed according to the modified method described in the literature[17]. Typically, 5 mL of $HAuCl_4$ solution (10 mM) was thoroughly mixed with 5 mL of Lyz solution (50 mg/mL) under vigorous stirring for 3 min. The pH of the mixed solution was then adjusted to about 11 by adding 1 M NaOH solution (1

mL). After reaction at 37 °C for 6 h at 500 rpm, a clear brown solution of Au NCs was obtained. After that, the solution of Lyz-Au NCs was filtered with a filter (pore size of 0.4 mm), and the filtrated solution was purified with a centrifugal ultrafiltration tube (Merck Millipore, MA, USA).

2.3 Synthesis of Lyz-Au NCs/RB conjugates

Lyz-Au NCs/RB conjugates were prepared through the interaction between Lyz and RB. 1 mL of RB solution (0.1mM) and 3mL, 1mL or 0.3mL Lyz-Au NC solution (0.1mM) were mixed, corresponding to Lys-Au NCs : RB = 3:1, 1:1, 0.3:1. Noted that the concentration of Lyz was regards as that of Lyz-Au NCs. The resultant solution was stirred at 500 rpm for 2 h using a magnetic stirrer. After that, the solution was purified with a centrifugal ultrafiltration tube to discard the free RB. After centrifuged ultrafiltration, the filtrate solution (<MW 3000) did not contain RB, indicating the binding of RB into the Lyz-Au NCs.

2.4 Detection of $^1O_2$

The $^1O_2$ generation by photoexcited Lyz-Au NCs/RB conjugate was evaluated with a chemical trap $^1O_2$ probe, MTX[18]. It is known that $^1O_2$ can selectively oxidize non-fluorescent MTX to form a fluorescent species. Typically, a 10 mM stock solution of MTX in DMF was prepared, and a 2 mL aqueous solution (D_2O) of the conjugates was then added to obtain a final concentration of MTX of 20 μM. The solutions were then irradiated with a white light-emitting diode (LED) (15 mW, 80 mW/cm^2 at 450 nm, SPF-D2, shodensha, Osaka, Japan) to detect $^1O_2$ generated by the conjugates.

The $^1O_2$ quantum yield of the Lyz-Au NCs/RB ($\Phi_{NC/RB}$) was calculated using the following equation

$$\Phi_{NC/RB} = \frac{\Phi_{RB} \times \Delta P_{NC/RB} \times A_{RB}}{\Delta P_{RB} \times A_{NC/RB}}$$

where $\Delta P_{NC/RB}$ and ΔP_{RB} are the fluorescence intensity change of MTX by Lyz-Au NCs/RB and RB, respectively. $A_{NC/RB}$ and A_{RB} represent the light absorbed by Lyz-Au NCs/RB and RB, respectively. A_{NC} and A_{RB} are determined by integration of the absorption bands in the wavelength range 400–800 nm. Φ_{RB} is the $^1O_2$ quantum yield of Rose Bengal, which is 0.75.

2.5 Absorption and fluorescence spectra

UV–Vis absorption spectroscopy and steady-state fluorescence spectroscopy measurements were conducted using a UV-vis-NIR spectrophotometer (V-670, JASCO,

Tokyo, Japan) and spectrofluorometer (FP-6300, JASCO)respectively. All the measurements were performed using 1 cm cuvettes at room temperature. Fluorescence lifetime was measured by time-correlated single photon counting with a Quantaurus-Tau fluorescence lifetime measurement system (C11367-03, Hamamatsu Photonics Co., Hamamatsu, Japan). Dynamic light scattering (DLS) was performed on a Zetasizer Nano ZS (Malvern Panalytical Ltd., Malvern, UK) equipped with a He–Ne laser operating at 632.8 nm and a scattering detector at 173°.

2.6 *Preparation of bacterial suspension*

Gram-positive facultative anaerobic bacteria, *S. mutans* ATCC 35668, *A. naeslundii* ATCC 27039, gram-negative facultative anaerobic bacteria, *E. coli* ATCC 25922, and gram-negative obligate anaerobic bacteria, *P. gingivalis* ATCC 63143627, *P. intermedia* ATCC 25611, were obtained from the American Type Culture Collection (Manassas, VA, USA) and kept frozen until analysis. The stocks were anaerobically incubated in brain heart infusion (BHI) broth (Pearlcore®, Eiken Chemical, Co., Ltd., Tokyo, Japan) for *E. coli*; supplemented with 0.1% antibiotic (gramicidin D and bacitracin, FUJIFILM Wako Pure Chemical Corporation) and 1% sucrose (FUJIFILM Wako Pure Chemical Corporation) for *S. mutans*; 0.5% yeast extract, 0.0005% hemin (Sigma-Aldrich Co. LLC St. Louis, MO, USA), and 0.0001% menadione (Sigma-Aldrich Co. LLC) for *P. gingivalis* and *P. intermedia*. Stock of *A. naeslundii* was incubated in actinomyces broth (Becton, Dickinson and Company, Franklin Lakes, NJ, USA). Anaerobic incubation was carried out in an Anaeropack system using anaerobic jars (Mitsubishi Gas Chemical Company, Inc., Tokyo, Japan).

2.7 Antibacterial effects of Lys-AuNCs/RB conjugate and white LED

For the antibacterial assessments, Lys-Au (0.23 μg/mL), Lys-AuNCs/RB (1 μg/mL) or RB (0.77 μg/mL) was added to a suspension containing *S. mutans* (final concentration: 5.5×10^6 colony-forming units (CFU) /mL) and white LED light irradiated for 1 min at a distance of 2 cm. Lys-Au NCs included Au at 25wt%, thus, we used the weight ratio of 1 : 4.3 : 3.3 (Lys-Au : Lys-Au NCs/RB : RB) to match the weigh content of Au NCs and RB. As control, *S. mutans* only received white LED light irradiation. After incubation for 24 h, the turbidity of each suspension was measured using a colorimeter (CO7500 Colourwave, Funakoshi Co., Ltd, Tokyo, Japan) at 590 nm. Subsequently, Lys-Au NCs/RB (0 (absence) and 1 μg/mL) were dissolved in the suspension of *S. mutans* (final concentration: 5.5×10^6 CFU/mL) and dispensed into microplates. This suspension was irradiated by white LED light for 1 min before incubation. After incubation for 24 h,

S. mutans suspensions were diluted 10-fold in fresh medium and spread onto blood agar medium (KYOKUTO Pharmaceutical Industrial, Co., Ltd, Sapporo, Japan). After incubation at 37°C for 24 h, *S. mutans* CFUs were determined.

To assess the antibacterial dose-dependent effect, Lys-Au NCs/RB conjugate (0 (absence), 0.01, 0.1, and 1 μg/mL) were dissolved in the suspension of *S. mutans* (final concentration: 5.5×10^6 CFU/mL) and dispensed into microplates. This suspension was irradiated by white LED light for 0 (no irradiation) or 1 min before incubation. After incubation for 24 h, the turbidity of each suspension was measured using a colorimeter at 590 nm. In addition, to examine the effect of light irradiation frequency, light irradiation of various exposure times, 0 (no irradiation), 30, and 60 s, was applied to *S. mutans* suspensions including Lys-Au NCs/RB (1 μg/mL), and then the bacterial turbidity was measured.

To examine the aPDT effects of Lys-Au NCs/RB conjugate on several types of bacterial strains, Lys-Au NCs/RB (0 (absence) and 1 μg/mL) were dissolved in the suspension of *E. coli* (5.5×10^6 CFU/mL), *A. naeslundii* (3.8×10^7 CFU/mL), *P. gingivalis* (2.8×10^{10} CFU/mL) and *P. intermedia* (1.1×10^7 CFU/mL), dispensed into microplates and then photoexcited for 1 min. After anaerobic incubation for 24 h, the turbidity of each suspension was measured using a colorimeter at 590 nm.

2.8 Morphological observations

Lys-Au NCs/RB conjugate (0 (absence) and 1 μg/mL) were dissolved in the suspension of *S. mutans* and photoexcited for 1 min. After incubation for 24 h, samples were fixed in 2.5% glutaraldehyde in 0.1 M sodium cacodylate buffer (pH 7.4) and then dehydrated in increasing concentrations of ethanol. After critical point drying and Pt-Pd coating, the samples were analyzed using scanning electron microscopy (SEM; S-4000, Hitachi Ltd., Tokyo, Japan) at an accelerating voltage of 10 kV. In addition, fixed samples were postfixed in 1% OsO_4 and 0.1 M sodium cacodylate buffer (pH 7.4) at 4°C for 1 h. Using the standard procedure, samples were dehydrated in ethanol, infiltrated with propylene oxide, and embedded in Epon. The samples were sliced and characterized using transmission electron microscopy (TEM; JEM-1400, JEOL Ltd., Tokyo, Japan) at 200 kV acceleration voltage.

2.9 Effect of Lys-AuNCs/RB conjugate on biofilm of S. mutans

The suspension of *S. mutans* (final concentration: 5.5×10^6 CFU/mL) was dispensed into microplates to produce the biofilm. After 24 or 48 h incubation, Lys-Au NCs/RB (0 (absence) and 1 μg/mL) were dropped onto *S. mutans* biofilm and then white LED light

irradiation for 1 min was carried out. Immediately, they were stained by the LIVE/DEAD BacLight Bacterial Viability Kit (Thermo Fisher Scientific, Waltham, MA, USA), according to the manufacturer's instructions. Live bacteria were stained with SYTO 9 to produce green fluorescence and bacteria with compromised membranes were stained with propidium iodide to produce red fluorescence. The bottom face of well of microplate were observed using fluorescence microscopy (BZ-9000 BioRevo, Keyence Corporation, Osaka, Japan). The fluorescence intensity was measured using software (ImageJ 1.41, National Institutes of Health, Bethesda, MD, USA).

2.10 Cytotoxic assessments

Fibroblastic NIH3T3 cells (RIKEN BioResource Center) was grown in 96-well plates using culture medium (MEM alpha, GlutaMAX-I, Thermo Fisher Scientific) supplemented with 10% fetal bovine serum (Qualified FBS, Thermo Fisher Scientific) and 1% antibiotics (Penicillin-Streptomycin, Thermo Fisher Scientific). Lys-Au NCs/RB conjugate (0 (absence), 0.01, 0.1, and 1 μg/mL) were added into the medium at final concentrations. Before incubation, suspensions were irradiated with white LED light for 1 min. The cultures were incubated at 37°C with 5% CO_2. As a control, non-irradiated suspensions were assessed. The cytotoxicity after incubation for 24 hours was determined using the WST-8 assay (Cell Counting Kit-8, Dojindo Laboratories, Mashiki, Japan) and lactate dehydrogenase (LDH) assay (Cytotoxicity LDH Assay Kit-WST, Dojindo Laboratories, Mashiki, Japan) following the manufacturer's instructions. The absorbance at 450 nm (WST-8) and 490 nm (LDH) was measured on a microplate reader (Multiskan FC, Thermo Fisher Scientific).

In addition, fluorescence observation *via* vinculin-F-actin double staining was performed. The cultured cells were washed with phosphate-buffered saline (PBS) and fixed with 3.5% formaldehyde in PBS for 5 min. After fixation and washing with PBS, cells were permeabilized with 0.5% Triton X-100 for 10 min and washed again with PBS. Then, cells were incubated for 30 min with BSA (7.5 w/v% Albumin Dulbecco's-PBS(-)Solution, from Bovine Serum, FUJIFILM Wako Pure Chemical Corporation Ltd.) as blocking buffer and washed with PBS. Next, 4 μL of 0.5 mg/mL anti-vinculin monoclonal antibody (Anti-Vinculin Alexa Fluor 488, eBioscience, San Diego, CA, USA) and 3 μL of 20 μg/mL phalloidin (Acti-stain 555 fluorescent Phalloidin, Cytoskeleton Inc., Denver, CO, USA) were diluted in 500 μL of methanol, 3 μL of 1 mg/mL DAPI solution (Dojindo Laboratories), and 500 μL of BSA, and the mixture was kept shaking for 1 h at 37°C. After standing for 1 day at 4°C, the sample was washed

three times with PBS (except for liquids) and then covered with a cover glass. The cells were observed using fluorescence microscopy.

Samples were stained using the LIVE/DEAD Viability/Cytotoxicity Kit for mammalian cells (Thermo Fisher Scientific), following the manufacturer's instructions. Live cells were stained with calcein acetoxymethyl to create green fluorescence, and cells with compromised membranes were stained with ethidium homodimer-1 to create red fluorescence. Stained samples were examined using fluorescence microscopy.

2.11 Statistical analysis

Statistical analysis was performed by Scheffe's test and student T-test. P values < 0.05 were considered statistically significant. All statistical procedures were performed using a software package (SPSS 11.0, IBM Corporation, Armonk, NY, USA).

3. Results and Discussion

3.1 Characterization of Lyz-Au NCs/RB conjugates

Fig.1A shows the absorption and fluorescence spectra of Lys-Au NCs, RB, and Lyz-Au NCs/RB conjugate. No apparent surface plasmon resonance absorption peak in 520 nm was observed for Lys-Au NCs, suggesting the formation of small Au NCs with the size less than 2 nm. It is well-know that large Au nanoparticles with the size of more than 3 nm show the surface plasmon resonance absorption peak. When excited at 370 nm, the solution of Lys-Au NCs showed an emission peak centered at 650 nm. The observation is consistent with the optical properties of Lys-Au NCs[19]. Upon conjugation of RB with Lyz-Au NCs, the RB absorption is observed at around 550 nm, in addition to the absorption of Lyz-Au NCs less than 450 nm; the absorbance of RB in the conjugates increases with the ratio of RB to Lyz-Au NCs (Fig.1B). This indicates the conjugation of Lyz-Au NCs and RB via the interaction of Lyz and RB[20] . The size (D) of Lyz-Au NCs/RB conjugate (Lyz-Au NCs: RB = 0.3:1) was estimated to be 12 nm using DLS measurement, which is larger than that of Lyz alone (D ~ 4 nm). This is because the formation of Lyz-Au NCs/RB conjugate.

3.2 RET process from Lyz-Au NCs to RB

The RET process from Lyz-Au NCs to RB is expected for this conjugate, since the donor (Lyz-Au NCs) emission and the acceptor (RB) absorption spectra are overlap[21]. The absorption spectrum of RB shows the absorption band at around 550 nm, which overlaps well with the emission spectrum of Lyz-Au NCs from 430 nm to 580 nm, satisfying this overlap condition of RET event. The fluorescent lifetime measurements

were conducted in order to confirm the occurrence of RET, i.e., a decrease in the average luminescence lifetime of the donor (Lyz-Au NCs). The analysis of the fluorescence time-resolved experiments was based on curve fitting methods as shown in Fig. 1C, and the results are summarized in Table 1. Herein, we monitored the fluorescence decay of Lyz-Au NCs at 650 nm at an excitation wavelength of 365 nm. As the ratio of RB to the Au NCs in the Lyz-Au NCs-RB conjugate increased, a decrease in the decay time of the Au NCs was observed, as shown in Fig. 1B. For example, the average decay time (~1.87 μs) of Lyz-Au NCs decreased to 0.29 μs for the Lyz-Au NCs/RB conjugate (0.3:1), accompanying a decrease in the fluorescence intensity of Au NCs, as shown in Fig. 1D. These observations suggest that the RET process occurs from the Au NCs to the RB in the Lyz-Au NCs/RB conjugate. Such RET process is expected to enhance the $^1O_2$ generation in the Lyz-Au NCs/RB conjugate[21].

3.3 $^1O_2$ generation by Lyz-Au NCs/RB conjugate under a white light LED

We evaluated the $^1O_2$ generation by photo-excited Lyz-Au NCs/RB conjugate with a chemical trap $^1O_2$ probe, MTX. The Lyz-Au NCs/RB conjugate has broad absorbance in the UV–Vis–NIR range, and hence a white-light LED was chosen as an effective photo-excitation source for the conjugate. The fluorescence spectra of MTX in the presence of the Lyz-Au NCs/RB conjugate in D_2O were acquired. The fluorescence intensities at 466 nm increased over time due to the oxidation of MTX by $^1O_2$ generated by the conjugate (Fig. 2). The increase of the fluorescence intensity under the light irradiation indicates the $^1O_2$ generation by photo-excited Lyz-Au NCs/RB conjugates. The $^1O_2$ quantum yield ($\Phi_{NC/RB}$) of Lyz-Au NCs/RB conjugates were estimated to be 0.20, 0.47, and 0.59 using RB ($^1O_2$ quantum yield $\Phi_{RB} = 0.75$) as a standard for Lyz-Au NCs:RB =3:1, 1:1, 0.3: 1 , respectively. At a higher RB ratio, the value of $^1O_2$ quantum yield increased. It is likely that the RET process from Au NCs to RB contributes to the enhanced $^1O_2$ generation by RB in the Lyz-Au NCs.

3.4 APDT and RET effects of Lys-Au NCs/RB conjugate

To assess the antibacterial effect of photoexcited Lys-Au NCs / RB conjugate, the turbidity of *S. mutans* suspension was measured to compare between Lys-Au NCs, Lys-Au NCs/RB or RB applied groups (Fig. 3A). Turbidity of control (absence), Lys-Au NCs, Lys-Au NCs/RB and RB was 0.49, 0.43, 0.13 and 0.37, respectively. The value of turbidity of Lys-Au NCs alone and RB alone was equivalent compared with control. In contrast, low turbidity was shown in photoexcited Lys-Au NCs/RB compared to other application groups ($p<0.01$). Assessment of CFU of *S. mutans* showed that application of

photoexcited Lys-Au NCs / RB significantly reduced the colony formation of *S. mutans* to 1/1000 when compared to no application of Lys-Au NCs/RB (Fig. 3B). From the results, it was suggested that Lys-Au NCs/RB photoexcited by white LED exerted antibacterial activity against *S. mutans*. We considered that photoexcited Au NCs and RB generated $^1O_2$ for the subsequent destructive effects. Oxidative stress mediated by reactive oxygen species (ROS) including $^1O_2$ causes some mechanisms to destroy bacterial cells. ROS stimulates lipid peroxidation to impair cell membrane functions and to produce toxic aldehydes through the attack to polyunsaturated fatty acids[22]. In addition, DNA replication was damaged by ROS activity regarding destroy the ligation moieties of nucleic acids, base and sugar groups[23].

In addition, we confirmed that antibacterial activity of Lys-Au NCs/RB conjugate was greater than RB alone, suggesting that RET event between Au NCs and RB was effectively provided in aPDT. White LED used for irradiation device is constructed by wide wavelength, 400 to 900 nm, and excite both Au NCs and RB. From the evidence when photoexcited Au NCs emitted the energy to transfer to RB (Fig. 1 and Table 1), $^1O_2$ production by RB was likely increased to up-regulate the antibacterial action. RET mechanism may potentiate the antibacterial effects and thus play a key role in development of future aPDT. Previous study reported the idea for enhancement of biological aPDT effects via RET. Yuan et al[24]. reported that the complex of luminol as the bioluminescence substrate and photosensitizer produced the RET to attack the bacterial cells and cancer cells[25]. RET system is anticipated to update of functionality of aPDT.

3.5 Dose- and time- dependent effect of aPDT using Lys-Au NCs/RB conjugate

To assess the dose dependent effect of aPDT using Lys-Au NCs/RB conjugate, the suspension of *S. mutans* received some concentrations of Lys-Au NCs/RB (0 (absence), 0.01, 0.1 and 1 μg/mL) with or without LED irradiation. In case of no irradiation, application of Lys-Au NCs/RB slightly decreased the turbidity of *S. mutans,* regardless of application concentration. With LED irradiation, turbidity of 0, 0.01, 0.1 and 1 μg/mL Lys-Au NCs/RB was 0.29, 0.28, 0.03 and 0.02, respectively. Photoexcited 0.1 and 1 μg/mL Lys-Au NCs/RB significantly decreased the turbidity of *S. mutans* (Fig. 3C). The results suggested that 0.1 μg/mL or greater Lys-Au NCs/RB was effective for aPDT. Previously, Miyata et al. evaluated the antibacterial activity of Au NCs ($Au_{25}(Capt)_{18}$) irradiated by blue LED[12]. They found that the suppression effect to *S. mutans* needed 500 μg/mL Au NCs. Thus, Lys-Au NCs/RB possibly exert the great antibacterial effect compared with Au NCs alone. We also speculated that the antibacterial activity of Lys-Au NCs/RB was derived from antibacterial protein Lyz, as well as organic dye, RB. Wu

et al. reported that antibacterial effects of chitosan nanoparticles was improved by adding the Lys[26].

To assess the time dependent effect of LED irradiation, *S. mutans* suspension with Lys-Au NCs/RB conjugate (0 (absence) and 1 μg / mL) received white LED irradiation for 0, 30, and 60 seconds. The result showed that each irradiation time significantly decreased the turbidity of *S. mutans* compared with control (absence of Lys-Au NCs/RB). In addition, 30 and 60 sec significantly diminished the turbidity compared to no irradiation sample (Fig. 3D). Hence, it was suggested that Lys-Au NCs/RB time-dependently enhanced the inhibitory effect to *S. mutans*. These results were supported by MTX examination which long term irradiation proceed the $^1O_2$ generation (Fig. 2).

3.6 Effect of photoexcited Lys-Au NCs/RB conjugate on several types of bacterial strains

Photoexcited Lys-Au NCs/RB conjugate consistently decreased the turbidity of several types of bacterial cells, *E. coli*, *A. naeslundii*, *P. gingivalis* and *P. intermedia*, compared with control (absence of Lys-Au NCs/RB) (Fig. 4A-D). Hence, it is likely that Lys-Au NCs/RB possess antibacterial activity to both gram negative and positive cells. *A. naeslundii* is known as primary colonizer of the tooth surface[27]. It is important the reduction of growth of primary colonizer related to dental biofilm formation to prevent the dental disease. *P. gingivalis* and *P. intermedia* are obligate anaerobic bacterium isolated from periodontitis and infected root canals[28,29]. They need to culture in anaerobic incubation condition, however, Lys-Au NCs/RB could show the reducing effect of turbidity of them despite of low residual oxygen. As mentioned above, antibacterial activity in anaerobic condition may be delivered from Lyz activity. It is expected that application of Lys-Au NCs/RB is effective in deep periodontal pocket and root canal, where the light dose not reach. However, further research is needed to elucidate about the relation between Lys-Au NCs/RB and residual oxygen.

3.7 Morphological observations

For morphologic assessments, we carried out the SEM and TEM observation to *S. mutans* applied with Lys-Au NCs/RB conjugate and LED irradiation (Fig. 5). SEM images of control (absence of Lys-Au NCs/RB) showed that chain of normally shaped *S. mutans* constructed bacterial colony. However, after Lys-Au NCs/RB and LED application, deformed bacterial cells were frequently found. In TEM images, of *S. mutans* of control (absence of Lys-Au NCs/RB) displayed spherical cell body enclosed by stable cell membrane. In contrast, cell body was frequently irregular with destruction of cell

membrane structure in Lys-Au NCs/RB and LED applied group. It was suggested that $^1O_2$ generated by photoexcited Lys-Au NCs/RB attack cell membrane consistently to reduce cell growth activity.

3.8 Suppression effect of photoexcited Lys-Au NCs/RB conjugate to bacterial biofilm

After application of photoexcited Lys-Au NCs/RB to *S. mutans* biofilm cultured for 24 and 48h, LIVE/DEAD BacLight staining frequently exhibited that bacterial cells stained in red, indicating dead cells. In contrast, control rarely showed *S. mutans* stained in red. (Fig. 6A). Quantify of LIVE/DEAD staining resulted in a significant increase in red ($P < 0.05$) compared with control (Fig. 6B). It was suggested that photoexcited Lys-Au NCs/RB was effective for bacterial biofilm. In dental therapy, destruction of bacterial biofilm is key point for attack inflammation disease, because antibiotics is not effective for biofilm[30]. In contrast to antibiotic therapy, some reports showed that aPDT destroy the bacterial cells in biofilm[31]. Pereira et al. revealed that MB dye and low-power laser succeeded the significant decreases in the viability of bacterial cells of in vitro biofilms[32]. Darabpour et al. also showed that Au NCs/MB conjugate exhibited significant anti-biofilm photoinactivation against *S. aureus*[33]. They speculated that MB dye was carried into deeper layers of biofilm. To fully realize aPDT to completely destroy biofilms, we consider that the combination of antibacterial and photosensitizing materials is important and further research is needed regarding nanotechnology and drug delivery[32].

3.9 Cytotoxic evaluation

WST-8 and LDH assay showed no significant difference between control (no application) and Lys-Au NCs/RB conjugate applied groups (Fig. 7A). Fluorescence observation of vinculin-F-actin double staining, associated with cell adhesion, revealed that cell shape of both control and aPDT groups was equivalent to normally spread on the culture dish (Fig. 7B upper). In the assessment of LIVE / DEAD staining, aPDT group showed cells stained with green fluorescence (live cells) as well as control group (Fig. 7B lower). Hence, it seemed likely that Lys-Au NCs/RB had the cell affinity. Normally, strong antibacterial activity frequently leads to strong cytotoxicity. Miyata et al. previously assessed that the biocompatible properties of Au NCs and conventional organic dye, MB, in clinical concentration setting[12]. The result showed that the viability of fibroblastic and osteoblastic cells was remarkably suppressed by MB, not Au NCs. In addition, RB is edible red dye and commonly used for plaque disclosing agents[34]. Biosafe properties of Lys-Au NCs/RB conjugate may be advantageous for medical application.

Conclusion

The antibacterial and cytocompatibility effects of Lys-AuNCs/RB conjugate photoexcited by white LED irradiation were investigated in vitro. Fluorescence measurements showed that $^1O_2$ was produced by photoexcited Lys-Au NCs/RB and RET process likely occur from the Au NCs to the RB in Lys-Au NCs/RB conjugate. The application of photoexcited Lys-Au NCs/RB significantly inhibited the growth of bacterial cells, such as *S. mutans, E. coli, A. naeslundii, P. gingivalis* and *P. intermedia.* Photoexcited Lys-Au NCs/RB provided the damage to *in vitro* biofilm of *S. mutans.* Furthermore, photoexcited Lys-Au NCs/RB showed low cytotoxicity against the NIH3T3 fibroblasts. Therefore, Lys-Au NCs/RB conjugate with white LED may be useful for aPDT of dental treatment.

Conflicts of interest

The authors have no conflict of interest to declare.

Acknowledgments

The authors acknowledge Hirofumi Miyaji, Saori Miyata, Kanako Shitomi, Tsutomu Sugaya (Department of Periodontology and Endodontology, Faculty of Dental Medicine, Hokkaido University), Natsumi Ushijima (Support Section for Education and Research, Faculty of Dental Medicine, Hokkaido University), Tsukasa Akasaka (Department of Biomedical, Dental Materials and Engineering, Faculty of Dental Medicine, Hokkaido University), Satoshi Enya and Hideya Kawasaki (Department of Chemistry and Materials Engineering, Faculty of Chemistry, Materials and Bioengineering, Kansai University) for their technical assistance in the assessments of Lys-Au NCs/RB conjugate. This work was supported by JSPS KAKENHI (19H02564). A part of this work was supported by the research grant of Tanaka Kikinzoku Memorial Foundation, Tokyo, Japan and the Akiyama Life Science Foundation Research Grant, Sapporo, Japan.

References

1) Davis JS, Jones CA, Cheng AC, Howden BP : Australia's response to the global threat of antimicrobial resistance: past, present and future. Med J Aust, 211(3) : 106-108, 2019.
2) Teirlinck E, Barras A, Liu J, Fraire JC, Lajunen T, Xiong R, Forier K, Li C, Urtti A, Boukherroub R, Szunerits S, De Smedt SC, Coenye T, Braeckmans K : Exploring Light-Sensitive Nanocarriers for Simultaneous Triggered Antibiotic Release and

Disruption of Biofilms Upon Generation of Laser-Induced Vapor Nanobubbles. Pharmaceutics, 11 : 201, 2019.
3) Wiehe A, O'Brien JM, Senge MO : Trends and targets in antiviral phototherapy. Photochem Photobiol Sci, 18 : 2565-2612, 2019.
4) Sperandio FF, Huang YY, Hamblin MR : Antimicrobial photodynamic therapy to kill Gram-negative bacteria. Recent Pat Antiinfect Drug Discov, 8 : 108-20, 2013.
5) Meisel P, Kocher T : Photodynamic therapy for periodontal diseases: state of the art. J Photochem Photobiol B, 79 : 159-70, 2005.
6) Biel MA : Photodynamic therapy of bacterial and fungal biofilm infections. Methods Mol Biol, 635 : 175-94, 2010.
7) Zanin IC, Gonçalves RB, Junior AB, Hope CK, Pratten J : Susceptibility of Streptococcus mutans biofilms to photodynamic therapy: an in vitro study. J Antimicrob Chemother, 56 : 324-30, 2005.
8) Wood S, Metcalf D, Devine D, Robinson C : Erythrosine is a potential photosensitizer for the photodynamic therapy of oral plaque biofilms. J Antimicrob Chemother, 57 : 680-4, 2006.
9) Konopka K, Goslinski T : Photodynamis therapy in dentistry. J Dent Res, 86 : 694-707. 2007.
10) Soria-Lozano P, Gilaberte Y, Paz-Cristobal MP, Pérez-Artiaga L, Lampaya-Pérez V, Aporta J, Pérez-Laguna V, García-Luque I, Revillo MJ, Rezusta A : In vitro effect photodynamic therapy with differents photosensitizers on cariogenic microorganisms. BMC Microbiol, 26 : 187, 2015.
11) Silva DF, Toledo Neto JL, Machado MF, Bochnia JR, Garcez AS, Foggiato AA : Effect of photodynamic therapy potentiated by ultrasonic chamber on decontamination of acrylic and titanium surfaces. Photodiagnosis Photodyn Ther, 27 : 345-353, 2019.
12) Miyata S, Miyaji H, Kawasaki H, Yamamoto M, Nishida E, Takita H, Akasaka T, Ushijima N, Iwanaga T, Sugaya T : Antimicrobial photodynamic activity and cytocompatibility of $Au_{25}(Capt)_{18}$ clusters photoexcited by blue LED light irradiation. Int J Nanomedicine, 12 : 2703-2716, 2017.
13) Ergin E, Dogan A, Parmaksiz M, Elçin AE, Elçin YM : Time-Resolved Fluorescence Resonance Energy Transfer [TR-FRET] Assays for Biochemical Processes. Curr Pharm Biotechnol, 17 : 1222-1230, 2016.
14) Yamamoto M, Shitomi K, Miyata S, Miyaji H, Aota H, Kawasaki H : Bovine serum albumin-capped gold nanoclusters conjugating with methylene blue for efficient $^1O_2$ generation via energy transfer. J Colloid Interface Sci, 510 : 221-227, 2018.

15) Jollès P, Jollès J : What's new in lysozyme research? Always a model system, today as yesterday. Mol Cell Biochem, 63 : 165-89, 1984.
16) Hukić M, Seljmo D, Ramovic A, Ibrišimović MA, Dogan S, Hukic J, Bojic EF : The Effect of Lysozyme on Reducing Biofilms by Staphylococcus aureus, Pseudomonas aeruginosa, and Gardnerella vaginalis: An In Vitro Examination. Microb Drug Resist, 24 : 353-358, 2018.
17) Xie J, Zheng Y, Ying JY : Protein-directed synthesis of highly fluorescent gold nanoclusters. J Am Chem Soc, 131 : 888-9, 2009.
18) Hirakawa K : Fluorometry of singlet oxygen generated via a photosensitized reaction using folic acid and methotrexate. Anal Bioanal Chem, 393 : 999-1005, 2009.
19) Lu D, Liu L, Li F, Shuang S, Li Y, Choi MM, Dong C : Lysozyme-stabilized gold nanoclusters as a novel fluorescence probe for cyanide recognition. Spectrochim Acta A Mol Biomol Spectrosc, 121 : 77-80, 2014.
20) ~~JW~~ Lafferty JW, ~~JR~~ Strande JR, ~~PM~~ Kerns PM, ~~NA~~ Fox NA, ~~S~~ Basu S : The interaction of photoactivators with proteins during microfabrication. Journal of Photochemistry and Photobiology A: Chemistry, 275 : 81-88, 2014.
21) Yamamoto M, Shitomi K, Miyata S, Miyaji H, Aota H, Kawasaki H : Bovine serum albumin-capped gold nanoclusters conjugating with methylene blue for efficient 1O2 generation via energy transfer. J Colloid Interface Sci, 510 : 221-227, 2018
22) Xiao M, Zhong H, Xia L, Tao Y, Yin H : Pathophysiology of mitochondrial lipid oxidation: Role of 4-hydroxynonenal (4-HNE) and other bioactive lipids in mitochondria. Free Radic Biol Med, 111 : 316-327, 2017.
23) Tan J, Duan M, Yadav T, Phoon L, Wang X, Zhang JM, Zou L, Lan L : An R-loop-initiated CSB-RAD52-POLD3 pathway suppresses ROS-induced telomeric DNA breaks. Nucleic Acids Res, in press, 2019.
24) Yuan H, Chong H, Wang B, Zhu C, Liu L, Yang Q, Lv F, Wang S : Chemical molecule-induced light-activated system for anticancer and antifungal activities. J Am Chem Soc, 134 : 13184-7, 2012.
25) Hsu CY, Chen CW, Yu HP, Lin YF, Lai PS : Bioluminescence resonance energy transfer using luciferase-immobilized quantum dots for self-illuminated photodynamic therapy. Biomaterials, 34 : 1204-12, 2013.
26) Wu T, Wu C, Fu S, Wang L, Yuan C, Chen S, Hu Y : Integration of lysozyme into chitosan nanoparticles for improving antibacterial activity. Carbohydr Polym, 155 : 192-200, 2017.

27) Li J, Helmerhorst EJ, Leone CW, Troxler RF, Yaskell T, Haffajee AD, Socransky SS, Oppenheim FG : Identification of early microbial colonizers in human dental biofilm. J Appl Microbiol, 97 : 1311-8, 2004.
28) Nakayama M, Ohara N : Molecular mechanisms of Porphyromonas gingivalis-host cell interaction on periodontal diseases. Jpn Dent Sci Rev, 53 : 134-140, 2017.
29) Nomura Y, Takeuchi H, Okamoto M, Sogabe K, Okada A, Hanada N : Chair-side detection of Prevotella Intermedia in mature dental plaque by its fluorescence. Photodiagnosis Photodyn Ther, 18 : 335-341, 2017.
30) Mah TF, O'Toole GA : Mechanisms of biofilm resistance to antimicrobial agents. Trends Microbiol, 9 : 34-9, 2001.
31) de Melo WC, Avci P, de Oliveira MN, Gupta A, Vecchio D, Sadasivam M, Chandran R, Huang YY, Yin R, Perussi LR, Tegos GP, Perussi JR, Dai T, Hamblin MR : Photodynamic inactivation of biofilm: taking a lightly colored approach to stubborn infection. Expert Rev Anti Infect Ther, 11 : 669-93, 2013.
32) Pereira CA, Romeiro RL, Costa AC, Machado AK, Junqueira JC, Jorge AO : Susceptibility of Candida albicans, Staphylococcus aureus, and Streptococcus mutans biofilms to photodynamic inactivation: an in vitro study. Lasers Med Sci, 26 : 341-8, 2011.
33) Darabpour E, Kashef N, Amini SM, Kharrazi S, Djavid GE : Fast and effective photodynamic inactivation of 4-day-old biofilm of methicillin-resistant Staphylococcus aureus using methylene blue-conjugated gold nanoparticles. Journal of Drug Delivery Science and Technology, 37 : 134-140, 2017.
34) Ishiyama K, Nakamura K, Ikai H, Kanno T, Kohno M, Sasaki K, Niwano Y : Bactericidal action of photogenerated singlet oxygen from photosensitizers used in plaque disclosing agents. PLoS One, 7 : 37871, 2012.

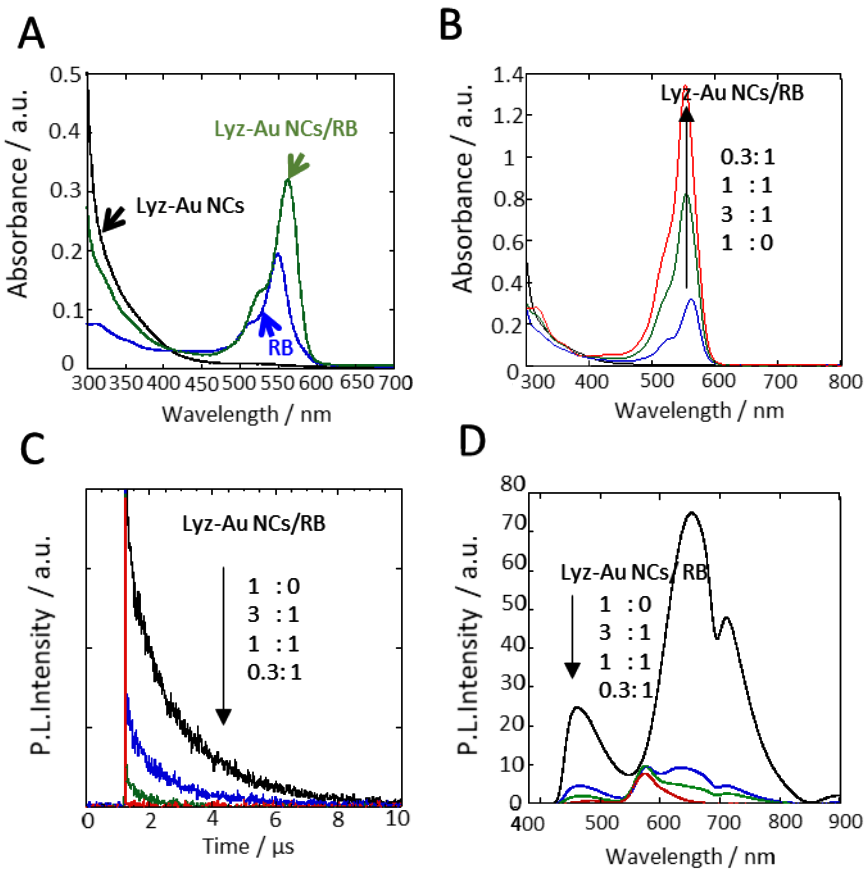
A
Absorbance / a.u.
Lyz-Au NCs/RB
Lyz-Au NCs
RB
Wavelength / nm
B
Absorbance / a.u.
Lyz-Au NCs/RB
0.3:1
1 :1
3 :1
1 :0
Wavelength / nm
C
P.L.Intensity / a.u.
Lyz-Au NCs/RB
1 :0
3 :1
1 :1
0.3:1
Time / μs
D
P.L.Intensity / a.u.
Lyz-Au NCs/ RB
1 :0
3 :1
1 :1
0.3:1
Wavelength / nm

Fig. 11

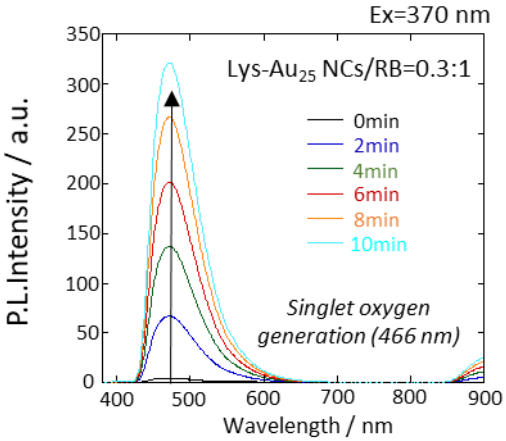
Ex=370 nm
Lys-Au25 NCs/RB=0.3:1
0min
2min
4min
6min
8min
10min
Singlet oxygen
generation (466 nm)
P.L.Intensity / a.u.
Wavelength / nm
350
300
250
200
150
100
50
0
400
500
600
700
800
900

Fig. 2

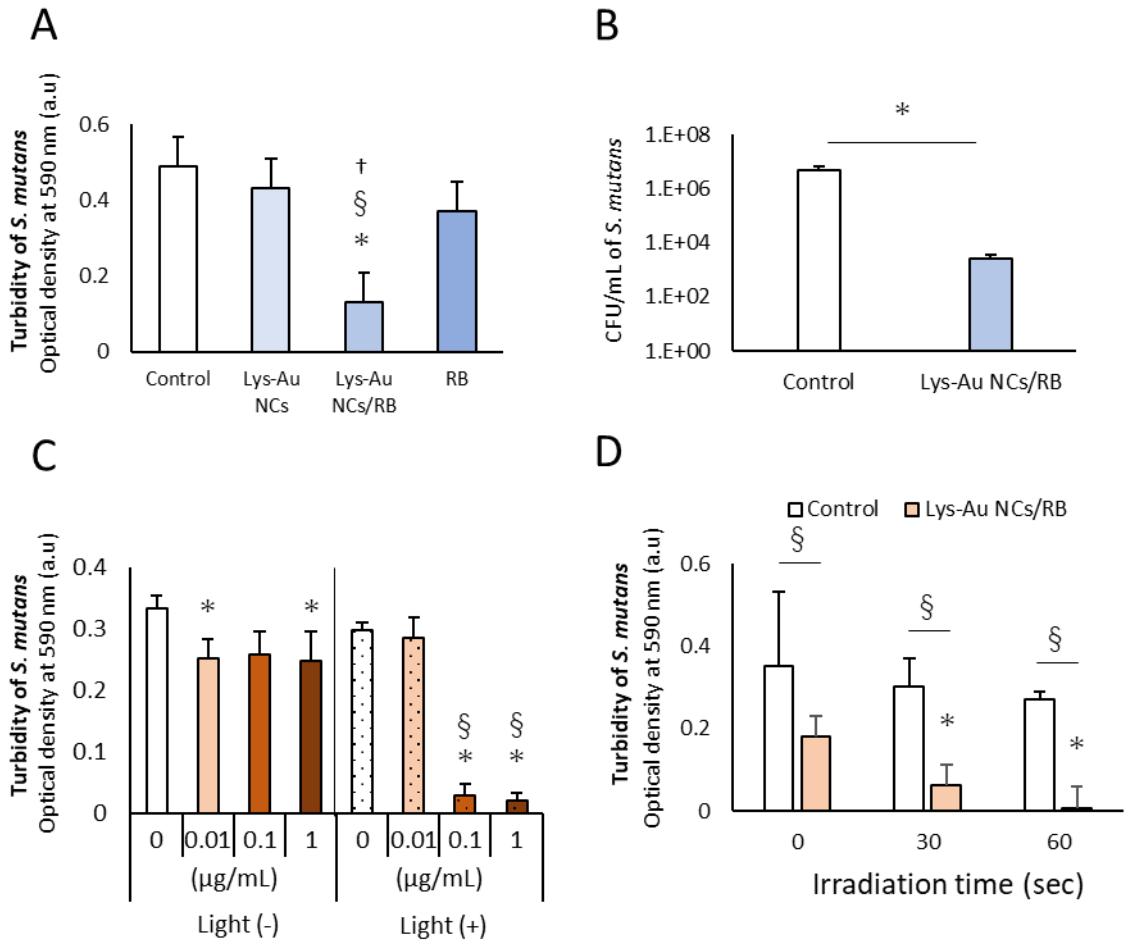
A
Turbidity of S. mutans
Optical density at 590 nm (a.u)
0.6
0.4
0.2
0
†
§
*
Control
Lys-Au NCs
Lys-Au NCs/RB
RB
B
CFU/mL of S. mutans
1.E+08
1.E+06
1.E+04
1.E+02
1.E+00
*
Control
Lys-Au NCs/RB
C
Turbidity of S. mutans
Optical density at 590 nm (a.u)
0.4
0.3
0.2
0.1
0
0
0.01
0.1
1
(μg/mL)
Light (-)
Light (+)
D
Control
Lys-Au NCs/RB
Turbidity of S. mutans
Optical density at 590 nm (a.u)
0.6
0.4
0.2
0
0
30
60
Irradiation time (sec)

Fig. 3

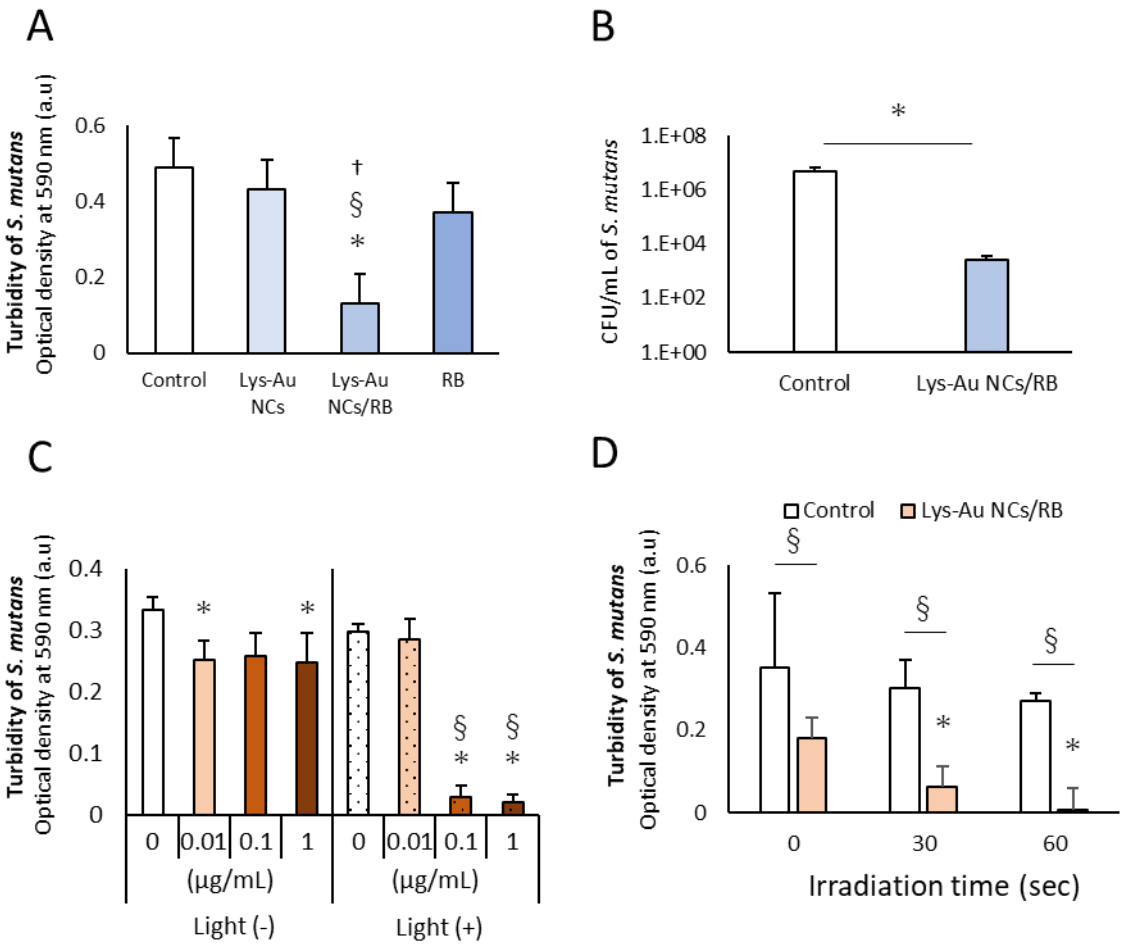
A
Turbidity of S. mutans
Optical density at 590 nm (a.u)
0.6
0.4
0.2
0
†
§
*
Control
Lys-Au NCs
Lys-Au NCs/RB
RB
B
CFU/mL of S. mutans
1.E+08
1.E+06
1.E+04
1.E+02
1.E+00
*
Control
Lys-Au NCs/RB
C
Turbidity of S. mutans
Optical density at 590 nm (a.u)
0.4
0.3
0.2
0.1
0
*
*
§
*
§
*
0
0.01
0.1
1
(μg/mL)
Light (-)
0
0.01
0.1
1
(μg/mL)
Light (+)
D
Control
Lys-Au NCs/RB
Turbidity of S. mutans
Optical density at 590 nm (a.u)
0.6
0.4
0.2
0
§
§
§
*
*
0
30
60
Irradiation time (sec)

Fig. 3

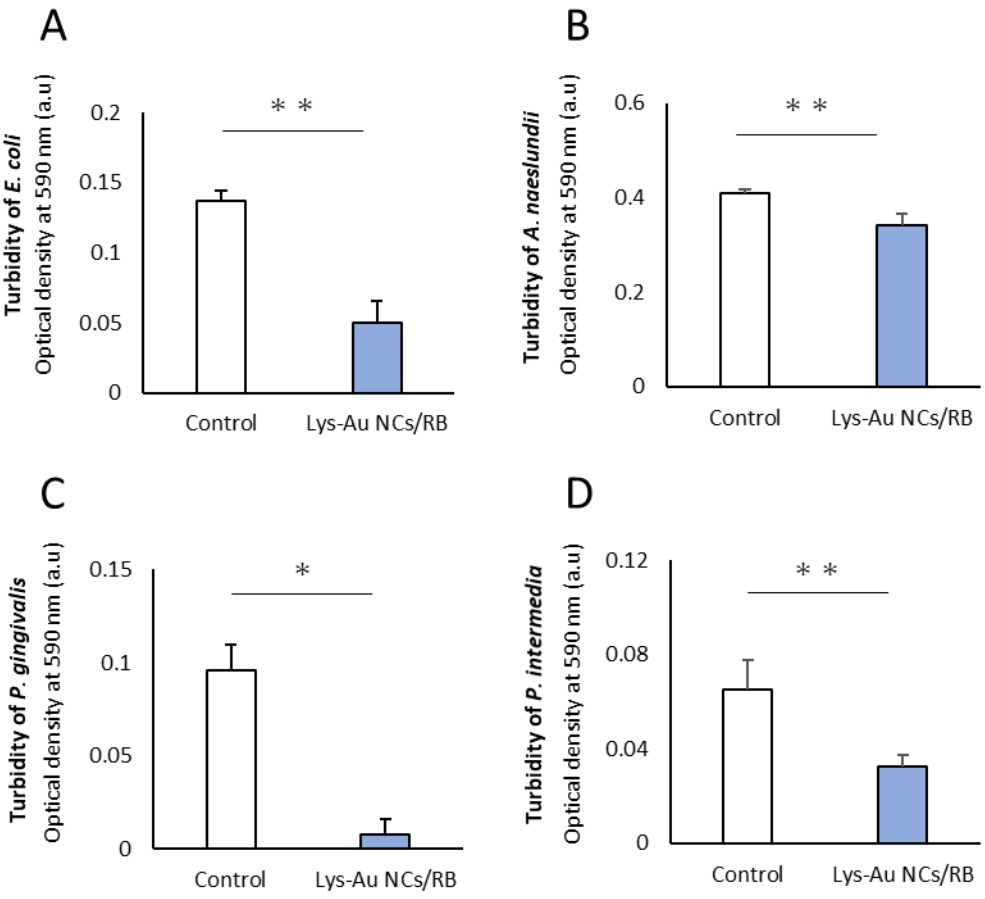
A
Turbidity of E. coli
Optical density at 590 nm (a.u)
0.2
0.15
0.1
0.05
0
* *
Control
Lys-Au NCs/RB
B
Turbidity of A. naeslundii
Optical density at 590 nm (a.u)
0.6
0.4
0.2
0
* *
Control
Lys-Au NCs/RB
C
Turbidity of P. gingivalis
Optical density at 590 nm (a.u)
0.15
0.1
0.05
0
*
Control
Lys-Au NCs/RB
D
Turbidity of P. intermedia
Optical density at 590 nm (a.u)
0.12
0.08
0.04
0
* *
Control
Lys-Au NCs/RB

Fig. 4

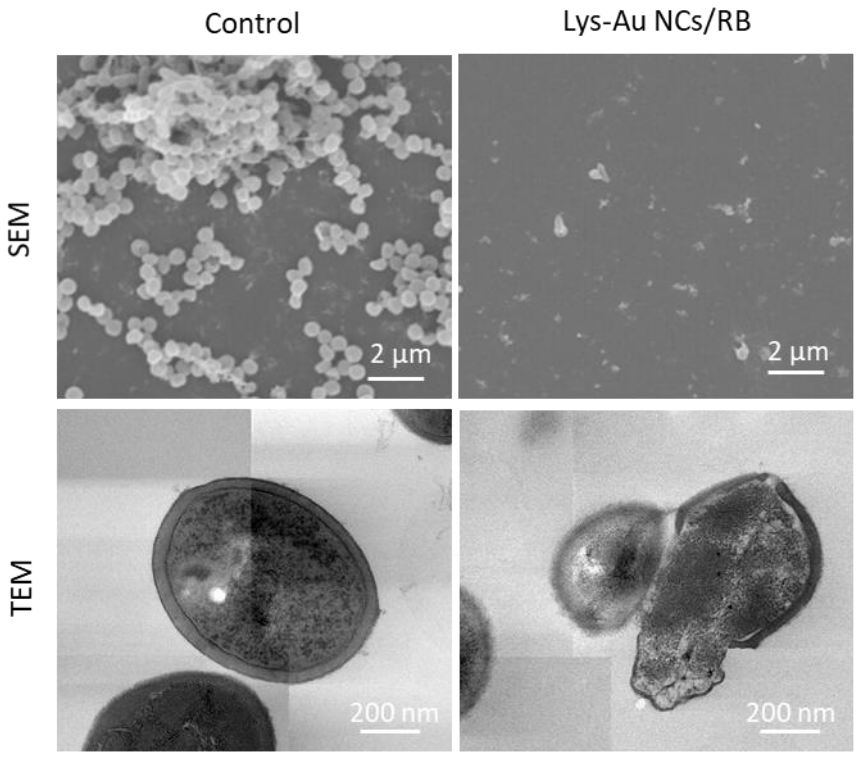

Fig. 5

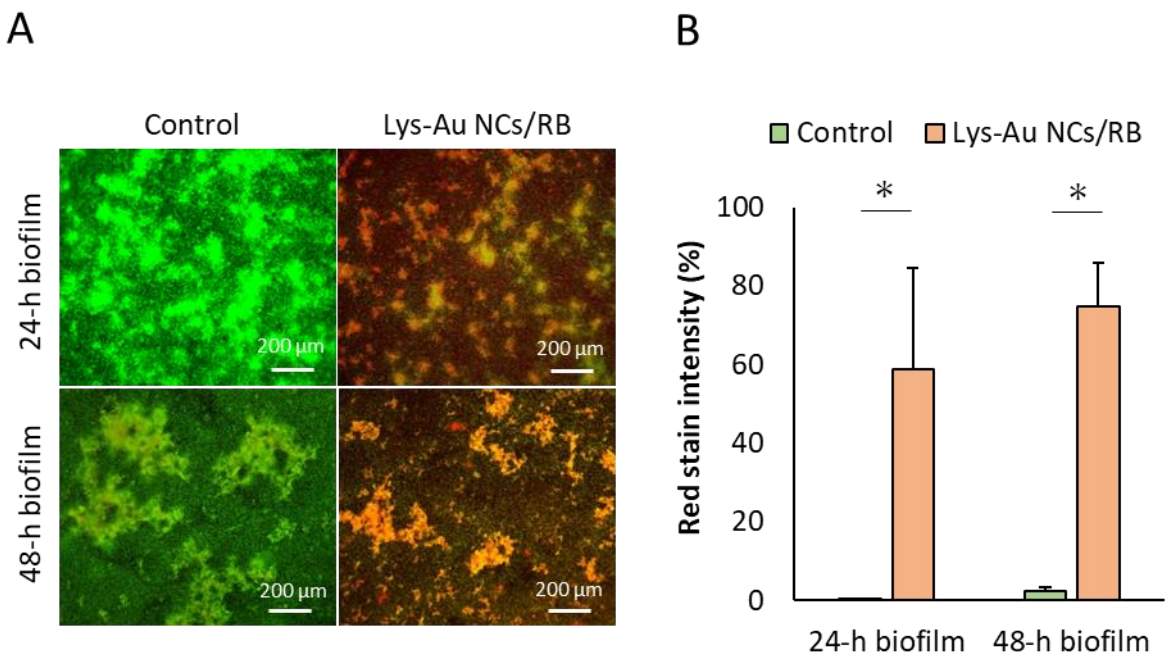
A
Control
Lys-Au NCs/RB
24-h biofilm
48-h biofilm
200 μm
200 μm
200 μm
200 μm
B
Control
Lys-Au NCs/RB
Red stain intensity (%)
100
80
60
40
20
0
*
*
24-h biofilm
48-h biofilm

Fig. 6

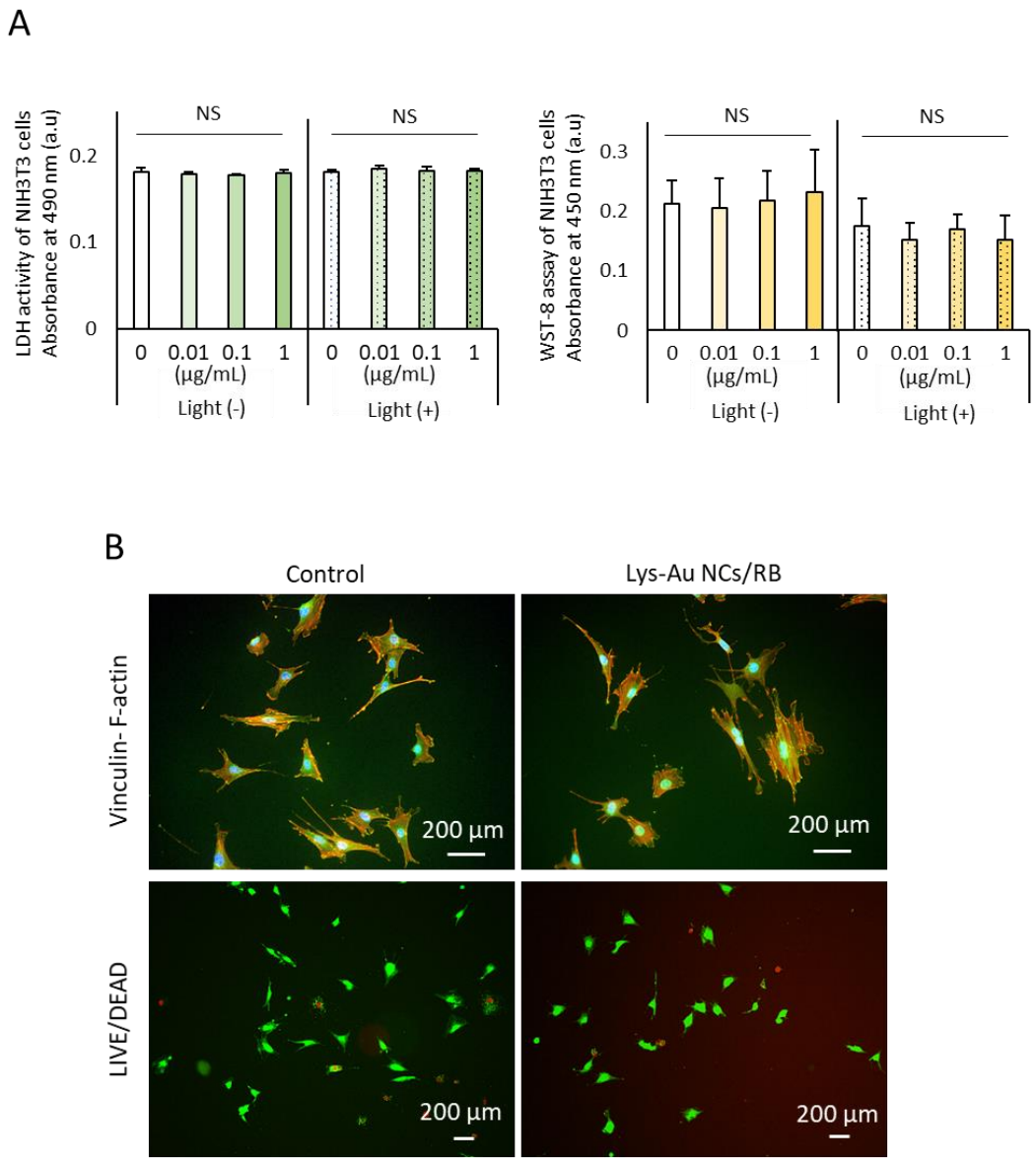
A
LDH activity of NIH3T3 cells
Absorbance at 490 nm (a.u)
0
0.1
0.2
NS
NS
0
0.01
0.1
1
(μg/mL)
Light (-)
Light (+)
WST-8 assay of NIH3T3 cells
Absorbance at 450 nm (a.u)
0
0.1
0.2
0.3
B
Control
Lys-Au NCs/RB
Vinculin- F-actin
LIVE/DEAD
200 μm

Fig. 7

Table.1 The parameters for Lyz-Au NCs and Lyz-Au NCs/RB conjugate.

entry	Em	<t>	$t_1(A_1)$	$t_2(A_2)$
Lys-AuNCs	650nm	1.87	0.475(0.37)	2.06(0.63)
(Au:RB) 3:1	650nm	1.38	0.009(0.88)	1.44(0.12)
(Au:RB) 1:1	650nm	0.66	0.052(0.95)	0.75(0.05)
(Au:RB) 0.3:1	650nm	0.29	0.003(0.99)	0.48(0.01)

τ_1 and τ_2 are the fluorescence lifetimes (μs), and $A_1 + A_2 = 1$.
$\langle\tau\rangle$ is the average fluorescence lifetime (μs).
Abbreviation : Lyz-Au NCs, lysozyme-Au nanoclusters; RB, rose bengal.

Table 1

Figure legends

Fig. 1. Characterization of Lys-AuNCs/RB conjugate

(A) UV–vis spectra of Lyz-Au NCs and Lyz-Au NCs/RB conjugate. (B) UV–vis spectra of Lyz-Au NCs and Lyz-Au NCs/RB conjugate with various ratios of Lyz-AuNCs to RB. (C) Fluorescence decay curves for Lyz-Au NCs and Lyz-Au NC/with various ratios of Lyz-AuNCs to RB at an excitation wavelength of 365 nm and an emission peak of 650 nm. (D) Fluorescence emission spectra of for Lyz-Au NCs and Lyz-Au NC/with various ratios of Lyz-Au NCs to RB at an excitation wavelength of 365 nm and an emission peak of 650 nm. Abbreviation : Lyz-Au NCs, lysozyme-Au nanoclusters; RB, rose bengal.

Fig. 2. Detection of $^1O_2$

Fluorescence spectra of MTX at an excitation wavelength of 370 nm in the presence of Lyz-Au NCs/RB conjugate (0.3:1) under white-light LED irradiation. Abbreviation : LED, light emitting diode; Lyz-Au NCs, lysozyme-Au nanoclusters; MTX, Methotrexate; RB, rose bengal.

Fig. 3. Antibacterial characterization of Lys-Au NCs/RB conjugate (mean± standard deviation)

(A) Turbidities of *S. mutans* of control, Lys-Au NCs, Lys-Au NCs/RB and RB groups (n=6): *, $P<0.01$ vs. control; §, $P<0.01$ vs. Lys-Au NCs; †, $P<0.01$ vs. RB. (B) CFU/mL of *S. mutans* of control and Lys-Au NCs/RB groups (n=3). (C) Turbidity of *S. mutans* with increasing dose of Lys-Au NCs/RB with or without LED irradiation (n=6): *, $P<0.01$ vs. 0 μg/mL; §, $P<0.01$ vs. 0.01 μg/mL. (D) Turbidity of *S. mutans* with increasing irradiation time (n=6): *, $P<0.05$ vs. 0 sec; §, $P<0.01$ vs. control. Abbreviation : CFU, colony forming unit; LED, light emitting diode; Lyz-Au NCs, lysozyme-Au nanoclusters; RB, rose bengal; *S. mutans*, *Streptococcus mutans*.

Fig. 4. Antibacterial activity of Lys-Au NCs/RB conjugate (mean± standard deviation)

Turbidities of *E. coli* (A), *A. naeslundii* (B), *P. gingivalis* (C) and *P. intermedia* (D) of control and Lys-Au NCs/RB groups (n=6). *, $P<0.05$; **, $P<0.01$. Abbreviation : *A. naeslundii*, *Actinomyces naeslundii*; *E. coli*, *Escherichia coli*; Lyz-Au NCs, lysozyme-Au nanoclusters; *P. gingivalis*, *Porphyromonas gingivalis*; *P. intermedia*, *Prevotella intermedia*; RB, rose bengal.

Fig. 5. Morphological examinations

SEM and TEM images of *S. mutans* of control and Lys-Au NCs/RB groups. Abbreviation : SEM, scanning electron microscope; TEM, transmission electron microscope; *S. mutans*, *Streptococcus mutans*; Lyz-Au NCs, lysozyme-Au nanoclusters; RB, rose bengal.

Fig. 6. LIVE/DEAD BacLight staining

(A) Fluorescence images of 24 and 48 h-incubated biofilms of *S. mutans* in control and Lys-Au NCs/RB groups. (B) Red stain intensity of *S. mutans* biofilms (n=3, mean± standard deviation). *, $P<0.05$. Abbreviation : Lyz-Au NCs, lysozyme-Au nanoclusters; RB, rose bengal; *S. mutans*, *Streptococcus mutans.*

Fig. 7. Cytotoxic assessments

(A) WST-8 and LDH activities of NIH3T3 cells with increasing dose of Lys-Au NCs/RB (n=6) (mean ± standard deviation). (B) Vinculin/F-actin staining and LIVE/DEAD BacLight staining of NIH3T3 cells in control and Lys-Au NCs/RB groups. Abbreviation : NS, not significant; LDH, lactate dehydrogenase; Lyz-Au NCs, lysozyme-Au nanoclusters; RB, rose bengal; WST-8, w~~W~~ater soluble tetrazolium salts-8.